A comparative study of implicit and explicit initialization for a tropical barotropic model

SUSMITA MAJUMDAR, D R C NAIR, R S SARASWAT, A CHANDRASEKAR

Department of Physics and Meteorology, Indian Institute of Technology, Kharagpur 721 302, India

The explicit nonlinear normal mode initialization (ENMI) scheme is applied to a tropical barotropic limited area shallow water model in spherical coordinates. The model is formulated by considering potential enstrophy conserving finite difference scheme. It is seen from the results of this study that the ENMI scheme is fully capable of filtering out the spurious gravity wave oscillations. The results are compared with those using an implicit nonlinear normal mode initialization (INMI). The latter scheme gives equally satisfactory results, requiring less computational time than the explicit scheme.

1. Introduction

Many numerical weather prediction models in current use are based on primitive equations. The primitive equations in general provide two different types of motion. One is the low-frequency meteorologically significant Rossby waves. The other contains the relatively high frequency gravity inertia waves, which are found to be a minor component of the observed atmospheric flow and are considered as *noise* in the forecast problem. Initialization is the process of filtering out the unwanted meteorological *noise* from the initial data and hence the above process provides a balanced initial state to the forecast model.

The nonlinear normal mode initialization (NMI), introduced by Machenhauer (1977), has been established as an efficient technique for the hemispheric and global numerical weather prediction models. Machenhauer suggested that the gravity wave oscillation could be removed by setting the initial time tendencies of gravity mode coefficients to zero keeping the Rossby mode coefficients unaltered. For global models this scheme was applied by Andersen (1977) and Daley (1979) with spectral version and by Temperton and Williamson (1981) with finite-difference version.

The success of NMI has naturally inspired a number of attempts to apply the above to a limited area model (LAM). In the conventional normal mode initialization, the horizontal modes are calculated explicitly to apply Machenhauer (1977) scheme. This technique is called *explicit nonlinear normal mode initialization* (ENMI). For global or hemispherical model, the normal modes can be formulated easily but difficulty arises in limited area model (Kasahara 1982). Briere (1982) proposed a method for implementing an initialization scheme for a barotropic as well as for a baroclinic version of a limited area model on a stereographic projection with constant coriolis parameter and constant map scale factor. Bijlsma and Hafkenscheid (1986) implemented the scheme to a baroclinic limited area model in spherical coordinates.

For certain limited area models, it is very difficult to know explicitly the spatial structure and the associated frequency of the normal mode. Bourke and McGregor (1983) have suggested a filtering scheme called vertical mode initialization technique which can be entirely expressed in physical space. Juvanon du Vachat (1986) established the connection between this method (scheme B) and Briere's scheme and showed that the horizontal structure mode could be expressed implicitly in terms of elliptic operator. Temperton (1988) developed a powerful technique called *implicit nonlinear normal mode initialization* (INMI) which does not require explicit knowledge of normal modes and therefore it can be performed in

Keywords. Limited-area shallow water model; nonlinear normal mode initialization (NMI); explicit nonlinear normal mode initialization (ENMI); implicit nonlinear normal mode initialization (INMI); potential enstrophy.

Proc. Indian Acad. Sci. (Earth Planet. Sci.), **106**, No. 3, September 1997, pp. 147–155

physical space rather than in normal mode space. Temperton applied this scheme to a barotropic version of finite element regional model (1988), to a barotropic global spectral model (1989) and to the multilevel finite element regional model (Temperton and Roch 1991). For a global spectral model, direct comparison of INMI and ENMI showed that the two schemes gave similar results; there were only small differences at the very largest horizontal scales (Temperton 1989). Though both the ENMI and INMI were implemented separately for LAM in several studies, a detailed comparison between these two schemes for LAM has not been done so far.

In this paper we present a comparative study of ENMI and INMI by using both the schemes to a shallow water tropical limited area model in spherical coordinates. For ENMI, the horizontal structure of normal modes is taken to be the eigen modes of the Laplacian operator, satisfying zero boundary conditions in the north-south (N-S) direction and the periodic boundary condition in the east-west (E-W) direction. Machenhauer's iteration algorithm for initialization is applied by taking the model variables in normal mode space. But INMI scheme is done in physical space by solving a number of Poisson and Helmholtz type partial differential equations.

After describing an outline of the shallow water model in section 2, section 3 describes briefly the explicit and implicit initialization schemes. Experimental results and discussions are provided in section 4. Finally the conclusions are included in section 5.

2. The model

The model is formulated by using shallow water equations in spherical coordinates. Horizontal discretization of the model equations is based on Sadourny's (1975) potential enstrophy conserving scheme. The staggering of the variables is done over an Arakawa-C grid. The nondimensional form of the model equations (with length scale = radius of the earth and time scale $= 1/2\Omega$, where Ω is the angular velocity of earth) can be written in semi-discretized form as follows:

$$\frac{\partial u}{\partial t} = \frac{-1}{\cos\theta}\delta_\lambda \phi + \overline{\eta}^{\theta}\overline{V}^{\lambda\theta} - \frac{1}{\cos\theta}\delta_\lambda K, \tag{1}$$

$$\frac{\partial v}{\partial t} = -\delta_\theta \phi - \overline{\eta}^{\lambda}\overline{U}^{\lambda\theta} - \delta_\theta K, \tag{2}$$

$$\frac{\partial \phi}{\partial t} = -\frac{\phi_0}{\cos\theta}[\delta_\lambda u + \delta_\theta(v\cos\theta)] - \frac{1}{\cos\theta}[\delta_\lambda(\overline{\phi'}^{\lambda} u) + \delta_\theta(\overline{\phi'}^{\theta} v\cos\theta)], \tag{3}$$

where u and v are the velocity components of the wind along zonal and meridional directions respectively, ϕ is the geopotential field and λ, θ are longitude and latitude respectively and

$$K = \tfrac{1}{2}[\overline{u^2}^{\lambda} + \overline{v^2}^{\theta}], \quad \phi' = \phi - \phi_o.$$

ϕ_o is the mean geopotential and $V = \overline{\phi}^{\theta} v$, $U = \overline{\phi}^{\lambda} u$. The potential vorticity η is defined as,

$$\eta = \left[\frac{1}{\cos\theta}\left(\frac{\partial v}{\partial \lambda} - \frac{\partial u\cos\theta}{\partial\theta}\right) + \sin\theta\right] \Big/ \overline{\phi}^{\lambda\theta}.$$

The operator δ denotes central difference quotient and is defined as follows. For any variable F,

$$\delta_\lambda(F) = \frac{F_{i+1/2,j} - F_{i-1/2,j}}{\Delta\lambda},$$

$$\delta_\theta(F) = \frac{F_{i,j+1/2} - F_{i,j-1/2}}{\Delta\theta}.$$

The over bars appearing in equations (1) - (3) denote average quantities of the variables with respect to λ or θ which are defined as follows,

$$\overline{F}^{\lambda} = \tfrac{1}{2}[F_{i+1/2,j} + F_{i-1/2,j}], \quad \overline{F}^{\theta} = \tfrac{1}{2}[F_{i,j+1/2} + F_{i,j-1/2}]$$

and $\overline{F}^{\lambda\theta}$ denotes the successive averaging with respect to λ and θ and this operation is commutative ($\overline{F}^{\lambda\theta} = \overline{F}^{\theta\lambda}$).

The choice of proper boundary condition is an important aspect of limited area modeling. Davies (1983) studied different boundary conditions for the limited area models and compared their performance. However for the present study the time invariant lateral boundary conditions are used. Here the prognostic variables u, v and ϕ are all kept time invariant along the boundary. Such boundary conditions can introduce noise near the boundary of the domain which can subsequently propagate towards the interior during integration of the model. To overcome the above a Laplacian type smoother is applied over the entire domain with the value of the smoothing coefficient increasing from the centre to the boundaries of the domain (Krishnamurti *et al* 1990).

3. Application of initialization to the model

The first step towards the normal mode initialization is the appropriate linearization of the shallow water system. Here we consider a simple linearization in spherical coordinates with a constant coriolis parameter f_0. β-terms are not considered here as they do not have any significant effect upon the initialized field (INMI) for our adopted domain (Nair 1993b). The domain, which we consider here extends from 7.5°S to 37.5°N and 54.375°E to 114.375°E consisting of 33×25 grid points with grid spacing $\Delta\lambda = \Delta\theta = 1.875°$. Nair showed that even for the above mentioned tropical domain, the INMI scheme produced no significant difference in the initialized field due to the addition of β-term in the linearization. Moreover since the main objective of this paper is the

comparison of implicit and explicit initialization and since the determination of normal modes after inclusion of all beta terms is complicated we have not considered β terms during linearization.

The shallow-water equations in vorticity and divergence form are given by

$$\frac{\partial \zeta}{\partial t} + f_0 D = Q_\psi, \tag{4}$$

$$\frac{\partial D}{\partial t} - f_0 \zeta + \nabla^2 \phi = Q_\chi, \tag{5}$$

$$\frac{\partial \phi}{\partial t} + \phi_o D = Q_\phi, \tag{6}$$

where

$$Q_\psi = -\left[\frac{\partial \psi}{\partial \lambda} + \cos\theta \frac{\partial \chi}{\partial \theta}\right] - [(\sin\theta - f_0)\nabla^2 \chi] - \frac{u}{\cos\theta}\frac{\partial(\nabla^2\psi)}{\partial \lambda} - v\frac{\partial(\nabla^2\psi)}{\partial\theta} - \nabla^2\psi\nabla^2\chi,$$

$$Q_\chi = -\left[\frac{\partial \chi}{\partial \lambda} - \cos\theta \frac{\partial \psi}{\partial \theta}\right] + [(\sin\theta - f_0)\nabla^2 \psi] + \frac{v}{\cos\theta}\frac{\partial}{\partial\lambda}(\nabla^2\psi) - u\frac{\partial}{\partial\theta}(\nabla^2\psi) + (\nabla^2\psi)^2 - \nabla^2\left(\frac{u^2+v^2}{2}\right),$$

$$Q_\phi = -\frac{1}{\cos^2\theta}\left[\frac{\partial}{\partial\lambda}(u\cos\theta\phi') + \cos\theta\frac{\partial}{\partial\theta}(v\cos\theta\phi')\right],$$

$$u = \frac{1}{\cos\theta}\left\{\frac{\partial\chi}{\partial\lambda} - \cos\theta\frac{\partial\psi}{\partial\theta}\right\},$$

$$v = \frac{1}{\cos\theta}\left\{\frac{\partial\psi}{\partial\lambda} + \cos\theta\frac{\partial\chi}{\partial\theta}\right\}.$$

The deviations from the coriolis parameter at the mean latitude of 15°N (f_0) have been absorbed into the first two terms of Q_ψ and Q_χ. The first term (in square bracket) of Q_ψ is nothing but $(-v\beta)$ and the corresponding term of Q_χ is nothing but $(-u\beta)$. The vertical component of vorticity, $\zeta = \nabla^2\psi$ and divergence, $D = \nabla^2\chi$ are defined in terms of ψ and χ which represent stream function and velocity potential, respectively. To find the normal modes of the model we set $Q_\psi = Q_\chi = Q_\phi = 0$ in equations (4)–(6). In the computation of INMI and ENMI, the boundary conditions are to be selected in such a way that the unwanted gravity modes should be suppressed. Here the boundary conditions are kept time invariant during initialization. In other words the changes of the dependent variables due to initialization $\Delta u, \Delta v$ and $\Delta\phi$ are all zero along the boundary. This set can form a consistent set of boundary conditions for initialization (Juvanon du Vachat 1988). The system can be written as

$$\frac{\partial}{\partial t}\begin{bmatrix}\zeta\\ D\\ \phi\end{bmatrix} - \begin{bmatrix}0 & -f_0 & 0\\ f_0 & 0 & -\nabla^2\\ 0 & -\phi_0 & 0\end{bmatrix}\begin{bmatrix}\zeta\\ D\\ \phi\end{bmatrix} = 0. \tag{7}$$

The eigen values and eigen vectors of the system can be derived from

$$\begin{bmatrix}0 & -f_0 & 0\\ f_0 & 0 & -\nabla^2\\ 0 & -\phi_0 & 0\end{bmatrix}\begin{bmatrix}\zeta\\ D\\ \phi\end{bmatrix} = \nu\begin{bmatrix}\zeta\\ D\\ \phi\end{bmatrix}. \tag{8}$$

The trivial solution for the eigen value $\nu = 0$ of the above system represents the slow modes for which we have, $f_0 D = 0$ i.e., $D = 0$ and $f_0\zeta - \nabla^2\phi = 0$. It shows that the slow modes are nondivergent and geostrophic. The nontrivial solution of $\nu \neq 0$ represents the fast modes and may be determined from (8) by eliminating ζ and D from the first and last equation,

$$[-f_0^2 + \phi_o\nabla^2]\phi = \nu^2\phi. \tag{9}$$

3.1 *Explicit initialization (ENMI)*

For explicit initialization equation (9) can be expressed as

$$\left[f_0^2 - \frac{\phi_0}{\cos^2\theta}\left(\frac{\partial^2}{\partial\lambda^2} + \cos\theta\frac{\partial}{\partial\theta}\cos\theta\frac{\partial}{\partial\theta}\right)\right]\phi = -\nu^2\phi. \tag{10}$$

The above equation is separable and the solution is of kind $\phi = \sin(\omega\lambda)F(\theta)$ (Juvanon du Vachat 1986). Considering a spherical domain $[\theta_0, \theta_1] \times [\lambda_0, \lambda_1]$ with $\omega = K\pi/\lambda_1 - \lambda_0$, K is an integer the equation (10) leads to an eigen value problem

$$\left[f_0^2 + \frac{\phi_0\omega^2}{\cos^2\theta}\right]F - \left[\frac{\phi_0}{\cos\theta}\frac{\partial}{\partial\theta}\cos\theta\frac{\partial}{\partial\theta}\right]F = -\nu^2 F, \tag{11}$$

with the boundary conditions $F(\theta_0) = F(\theta_1) = 0$. The normalized Rossby mode and eastward and westward gravity modes are given by [cf. Briere (1982), Bijlsma and Hafkenscheid (1986)]

$$P_{kl1} = A_{kl1}\sigma_{kl}^{-1}S_{kl}(i,j),$$

$$P_{klr} = A_{klr}(\alpha_{kl}\sigma_{kl})^{-1}(2\phi_0)^{-1/2}S_{kl}(i,j), \quad r = 2,3,$$

where

$$A_{kl1} = (0, 1, f_0)^T,$$

$$A_{klr} = (\nu_{klr}, f_0, -\alpha_{kl}^2\phi_0)^T, \quad r = 2,3$$

and where $S_{kl}(i,j)$ and $(-\alpha_{kl}^2)$ are the eigen functions and eigen values of the discrete Laplacian operator.

Here $\nu_{kl1} = 0$ corresponds to the Rossby wave, while $\nu_{kl2} = i\sigma_{kl}$, $\nu_{kl3} = -i\sigma_{kl}$ where $\sigma_{kl} = (\alpha_{kl}^2\phi_0 + f_0^2)^{1/2}$ corresponds to the fast gravity waves which move eastward and westward.

The normal mode expansion of $\hat{\eta}(i,j) = (\chi(i,j), \psi(i,j), \phi(i,j))^T$ can be written as

$$\hat{\eta}(i,j) = \sum_{k=1}^{m}\sum_{l=1}^{n}\sum_{r=1}^{3}\hat{\gamma}_{klr}P_{klr}, \quad \text{where } \hat{\gamma}_{klr} = \langle\hat{\eta}, P_{klr}\rangle.$$

Then projecting the nonlinear form of equations (4)–(6) on gravity wave components and setting the initial

tendencies of the gravity wave components to zero the increments of the spectral coefficient are given by [cf. Bijlsma and Hafkenscheid 1986]

$$\Delta\chi_{kl} = -\frac{f_0}{\sigma_{kl}^2 \alpha_{kl}^2}\left(\frac{\partial}{\partial t}\nabla^2\psi\right)_{kl} - \frac{1}{\sigma_{kl}^2}\left(\frac{\partial\phi}{\partial t}\right)_{kl},$$

$$\Delta\psi_{kl} = \frac{f_0}{\sigma_{kl}^2 \alpha_{kl}^2}\left(\frac{\partial}{\partial t}\nabla^2\chi\right)_{kl},$$

$$\Delta\phi_{kl} = -\frac{\phi_0}{\sigma_{kl}^2}\left(\frac{\partial}{\partial t}\nabla^2\chi\right)_{kl}.$$

A transformation of these increments back to real space leads to corrections which are applied to the fields. The improvements of wind fields can be calculated by solving

$$\nabla^2(\Delta\chi) = \Delta D \quad \text{and} \quad \nabla^2(\Delta\psi) = \Delta\zeta, \tag{12}$$

and then by using the above solutions in the following equations

$$\Delta u = \frac{1}{\cos\theta}\left[-\cos\theta\frac{\partial\Delta\psi}{\partial\theta} + \frac{\partial\Delta\chi}{\partial\lambda}\right], \tag{13}$$

$$\Delta v = \frac{1}{\cos\theta}\left[\frac{\partial\Delta\psi}{\partial\lambda} + \cos\theta\frac{\partial\Delta\chi}{\partial\theta}\right]. \tag{14}$$

At any iterative step q the values of the prognostic variables are modified $u^{q+1} = u^q + \Delta u$, $v^{q+1} = v^q + \Delta v$ and $\phi^{q+1} = \phi^q + \Delta\phi$.

3.2 *Implicit initialization (INMI)*

For models with definite geometry and complicated boundary conditions the above scheme may not be applicable. Now by eliminating D from the first and last equations in the system (8), we get $\zeta\phi_o - f_0\phi = 0$, and this shows that the linearized potential vorticity is zero. Apart from the orthogonality of the modes, we can conclude two important properties of the modes (Temperton 1988) viz., the slow modes are stationary and non-divergent (i.e., $D_R = 0$ and $\nabla^2\phi_R = f_0\zeta_R$) and the fast modes have zero linearized potential vorticity (i.e., $\phi_o\zeta_G - f_0\phi_G = 0$).

Now the equation (4.25) of Temperton (1988) takes the form

$$\begin{bmatrix} 0 & f_0 & 0 \\ -f_0 & 0 & \nabla^2 \\ 0 & \phi_0 & 0 \end{bmatrix}\begin{bmatrix} \Delta\zeta \\ \Delta D \\ \Delta\phi \end{bmatrix} = \begin{bmatrix} \delta_t\zeta \\ \delta_t D \\ \delta_t\phi \end{bmatrix}_G, \tag{15}$$

where δ_t is the forward time difference operator and $\Delta\zeta, \Delta D, \Delta\phi$ are the required changes (corrections) of the model variables ζ, D and ϕ. The subscript G denotes the fast mode component of the vector. The tendency of the observed field is obtained by running the model for one time step forward.

$$\delta_t F = \frac{F(t = \Delta t) - F(t = 0)}{\Delta t}. \tag{16}$$

The tendency of the 'observed' or analyzed field can be partitioned as $(\delta_t X)_O \equiv (\delta_t X)_R + (\delta_t X)_G$. By using the above mentioned properties the 2nd equation of the system (15) becomes

$$\left[\nabla^2 - \frac{f_0^2}{\phi_o}\right](\Delta\phi) = (\delta_t D)_O, \tag{17}$$

from which $\Delta\phi$ can be estimated and the corresponding change, $\Delta\zeta$ can be found from 2nd property,

$$\Delta\zeta = \frac{f_0\Delta\phi}{\phi_o}. \tag{18}$$

The 3rd equation of the system (15) is

$$\phi_o\Delta D = (\delta_t\phi)_G. \tag{19}$$

Using 1st and 2nd property

$$\left[\nabla^2 - \frac{f_0^2}{\phi_o}\right](\delta_t\phi)_G = \nabla^2(\delta_t\phi)_O - f(\delta_t\zeta)_O. \tag{20}$$

Once $(\delta_t\phi)_G$ has been found, the required change ΔD is given by (19)

The improvements u and v can be calculated by using the equations (12–14).

4. Results and discussions

The domain of integration extends from 7.5°S to 37.5°N and 54.375°E to 114.375°E. The experiments have been performed using the basic data extracted from FGGE IIIb data set for a typical monsoon depression at 12 UTC (500 hPa), 6th July of 1979. The domain consists of 33×25 grid points with $\Delta\lambda = \Delta\theta = 1.875°$. The mean depth of the fluid at 500 hPa is taken as 5700 m. The model is integrated for 24 hours with a time step, $\Delta t = 3$ minutes. The integration begins with a forward time step followed by subsequent leapfrog time steps. A Robert time filter is used (Nair *et al* 1993a) to avoid the computational mode associated with the leapfrog scheme.

The numerical experiments are carried out with explicit nonlinear normal mode initialization (ENMI), with implicit nonlinear normal mode initialization (INMI) and without initialization (NOIN). It is customary in limited area models to consider the domain of integration to be larger than the domain of interest and use the latter to interpret the results. We have followed the above and hence have considered the following domain of interest (61.875°E to 106.875°E and 0° to 30°N). The results of this study are depicted over the domain of interest only.

4.1 *Removal of high frequency noise from the forecast*

The primary goal of the initialization is the removal of spurious high-frequency noise from the forecast. In

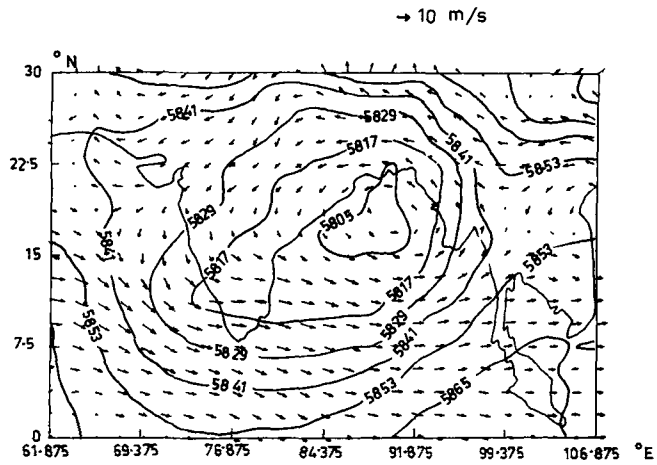

Figure 1. Initial input wind and height analysis fields at 500 mb on July 6th, 1979 (12 UTC).

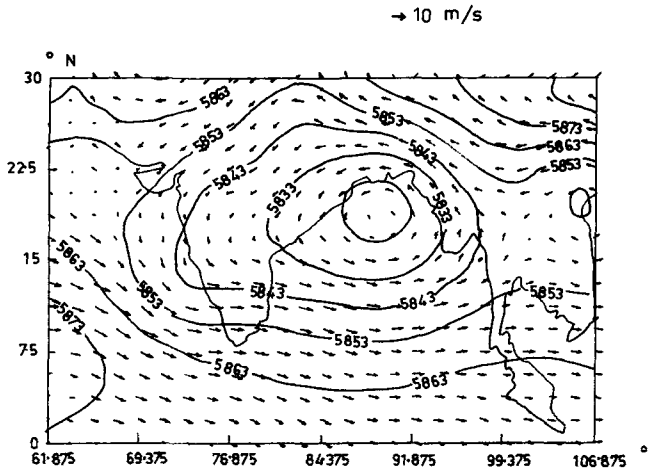

Figure 2. Initialized (explicit) wind and height fields at 500 mb on July 6th, 1979 (12 UTC).

figure 1, the initial input analysis fields are shown at 12 UTC (6th July, 1979). The centre of depression over the Bay of Bengal lies at (16.875°N, 90°E). The circulation centre remains unaltered during explicit initialization process (as shown in figure 2) with only a change in the height field (approx. 10 m). As compared to the basic input fields, the initialized fields are very smooth and ensure balance between wind and mass fields.

The height field forecast for the first 24 hrs of the three runs (NOIN, ENMI and INMI) may be seen at two selected grid points; one at 71.25°E, 9.375°N (figure 3) and the other almost at the center of the domain 80.625°E, 18.75°N (figure 4). Solid line indicates uninitialized prediction (NOIN), dashed line indicates prediction after explicit initialization (ENMI) while the line indicated by box shows prediction after implicit initialization (INMI). The noisy character of the uninitialized forecast and the capability of initialization (both ENMI & INMI) in

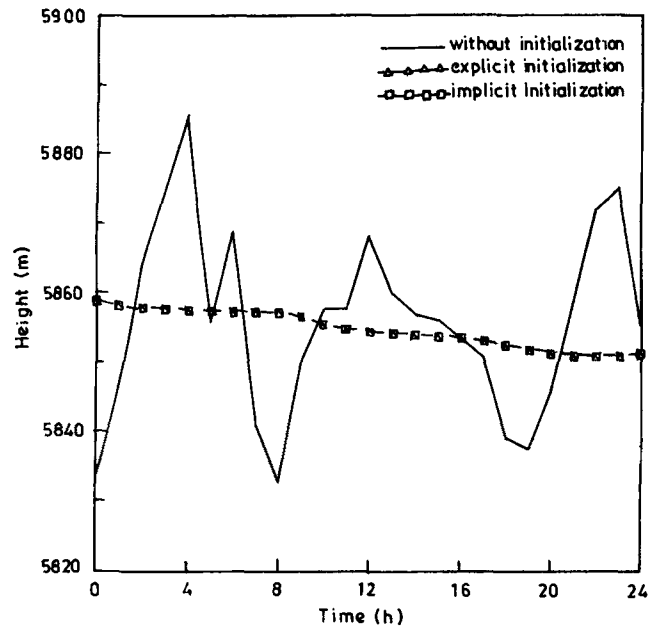

Figure 3. Time variation of height (m) fields at (71.25°E, 9.375°N).

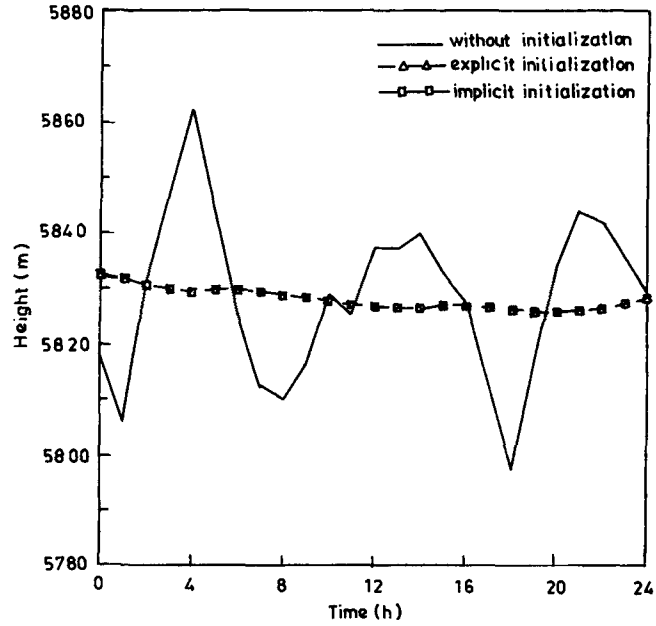

Figure 4. Time variation of height (m) fields nearer to the centre of the domain (80.625°E, 18.75°N).

filtering out the gravity wave oscillation is very clearly brought out by figures 3 and 4.

A useful global measure of gravity wave activity is the mean divergence defined by

$$N_1 = \left(\frac{1}{mn}\right) \sum_{i=1}^{m} \sum_{j=1}^{n} |(\nabla.V)_{ij}|.$$

The evolution of N_1 is plotted in figure 5 for the three parallel forecasts. In NOIN, N_1 has an initial value of almost $3 \times 10^{-6}\ S^{-1}$ and decreases during the forecast

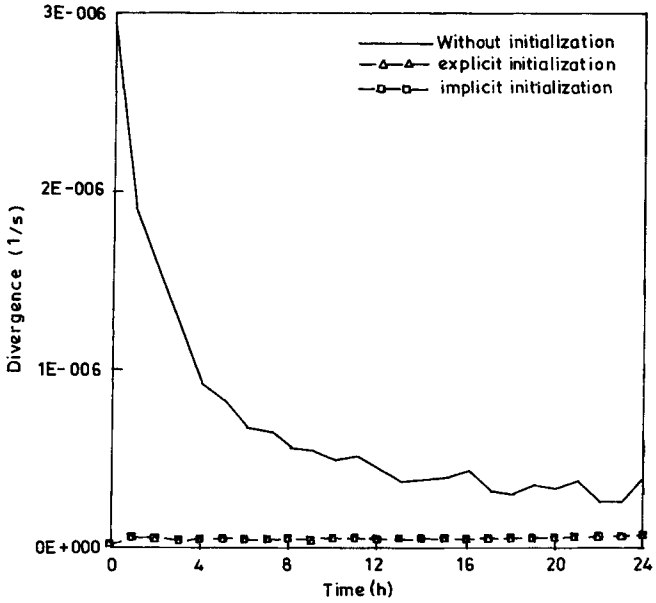

Figure 5. Time variation of mean absolute divergence (1/s).

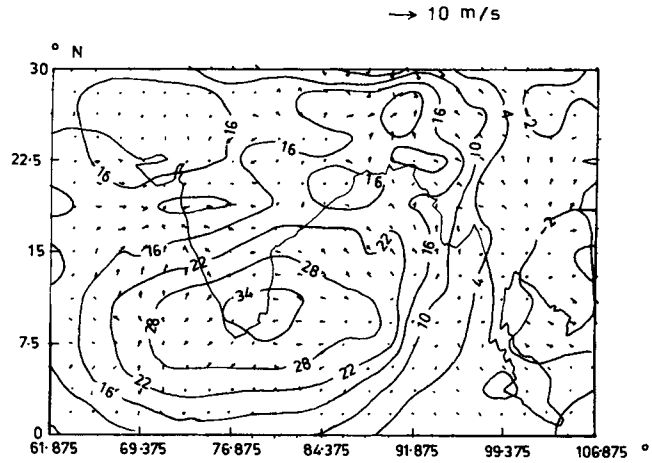

Figure 6. Difference in wind and height fields between initialized (explicit) and uninitialized fields at 500 mb on July 6th, 1979 (12 UTC).

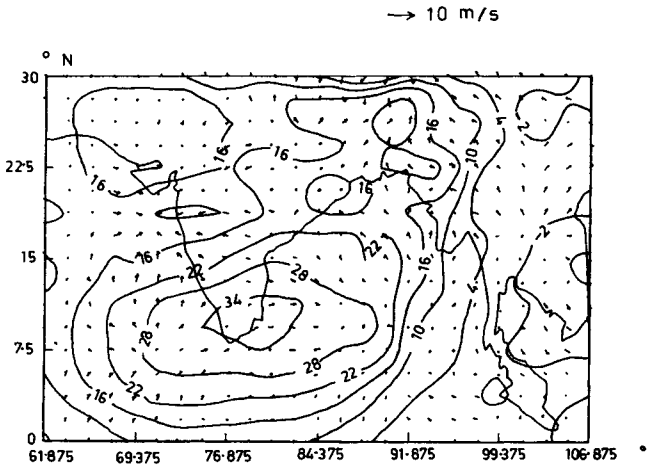

Figure 7. Difference in wind and height fields between initialized (implicit) and uninitialized fields at 500 mb on July 6th, 1979 (12 UTC).

due to various smoothing processes in the model reaching almost to an asymptotic value of $4 \times 10^{-7} S^{-1}$ after 12 hours. Both ENMI and INMI schemes reduce the initial value of N_1 to $10^{-8} S^{-1}$ which then remains more or less steady.

4.2 *Changes in the initial fields*

An important requirement of any initialization procedure is that the changes made in the initial data be acceptably small. To ensure that the analysis is not degraded by the initialization, the root-mean-square (rms) changes made to the initial fields of height and wind components by the ENMI and INMI schemes averaged over the entire domain are tabulated in the first column of table 1. The changes are small in magnitude and are very similar for ENMI and INMI.

The differences of the initialized height and wind fields from the uninitialized fields at the start of the forecast for both schemes (ENMI and INMI) are shown in figures (6) and (7). The height difference fields are smooth, attain maximum at the same point (80.625°E, 11.25°N) and have almost the same value

Table 1. *Root-mean-square (rms) differences between the initialized and uninitialized wind components and height fields. The differences are averaged over the entire domain. The entries in the first column are the differences at $t = 0$. The entries in the other columns refer to the differences at $t = 12$ hrs. The second column shows the differences in the forecast fields with one iteration of initialization schemes, the third column with two iterations and the fourth column with three iterations.*

r.m.s. difference		At $t = 0$	At $t = 12$ hours		
			One iteration	Two iterations	Three iterations
u (m/s)	INMI-NOIN	0.02423	0.00876	0.00878	0.00874
	ENMI-NOIN	0.0251	0.00931	0.00913	0.00913
v (m/s)	INMI-NOIN	0.02871	0.0103	0.009	0.0098
	ENMI-NOIN	0.02844	0.0101	0.00987	0.00988
h (m)	INMI-NOIN	0.42486	0.32031	0.3269	0.32606
	ENMI-NOIN	0.42137	0.3318	0.3276	0.3276

Table 2. *Maximum (max.) differences in wind components and height between the initialized (with two iterations) and uninitialized analysis. (INMI-NOIN): changes due to implicit initialization; (ENMI-NOIN): changes due to explicit initialization. Entries in the first, second and third columns show the max differences at $t = 0$, $t = 12$ hrs and $t = 24$ hrs respectively.*

Max. difference		At $t = 0$	At 12 hrs	At 24 hrs
u (m/s)	INMI-NOIN	4.5709	0.9850	0.8768
	ENMI-NOIN	4.8585	1.0226	0.8380
v (m/s)	INMI-NOIN	3.9483	0.7588	0.9363
	ENMI-NOIN	3.4609	0.9298	0.8653
h (m)	INMI-NOIN	36.1624	9.6089	5.5004
	ENMI-NOIN	35.8640	9.7270	5.3339

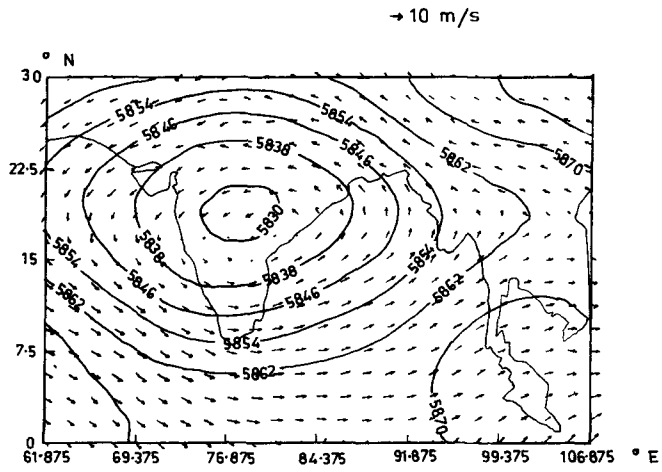

Figure 8. 24-hour forecast of wind and height fields starting from the uninitialized data at 500 mb on July 6th, 1979 (12 UTC).

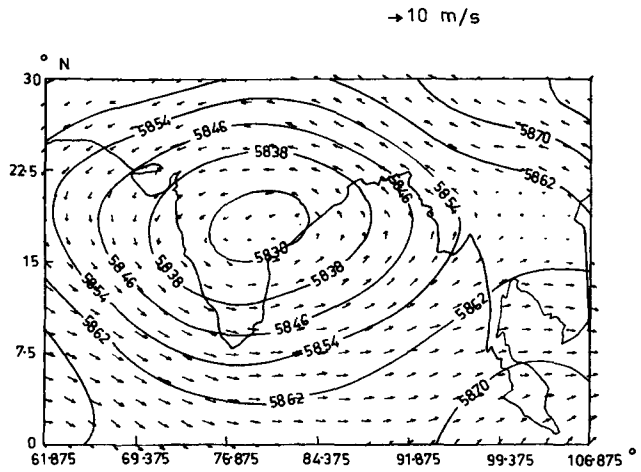

Figure 10. 24-hour forecast of wind and height fields starting from INMI data at 500 mb on July 6th, 1979 (12 UTC).

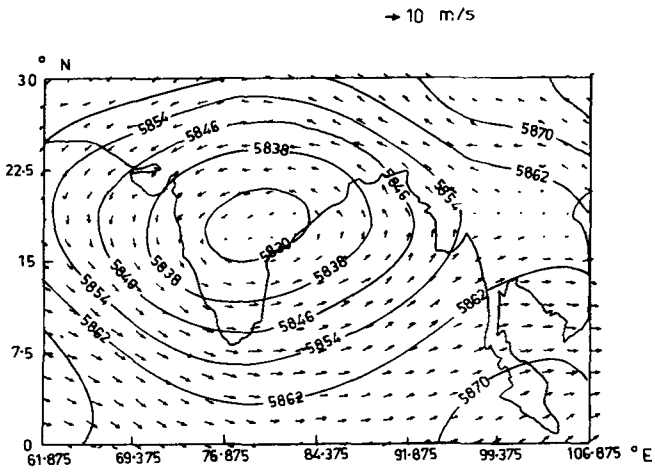

Figure 9. 24-hour forecast of wind and height fields starting from ENMI data at 500 mb on July 6th, 1979 (12 UTC).

for both the schemes. It is hard to detect any differences between the two figures.

4.3 *Changes in the forecasts*

In order to examine the impacts of initialization on short range prediction three parallel model integrations (with uninitialized , ENMI and INMI data sets) are made. Initialization schemes are incorporated only at the start of the forecast.

In order to compare the impact of the initialization scheme on prediction in a quantitative manner, the rms differences and the maximum differences of the height and wind components between the initialized (ENMI and INMI) and the uninitialized data are shown in table 1 and table 2, respectively. In table 1, the second, third and fourth columns represent the rms differences averaged over the entire domain at 12 hours with one, two and three iterations of initialization schemes. The changes at 12 hours are seen to have decreased markedly compared to the initial difference values (first column of table 1). Moreover, the rms differences are very similar in ENMI and INMI cases and do not change significantly from iteration to iteration. The first, second and third columns of table 2 represent the maximum differences between the initialized and uninitialized data initially, at 12 hours and at 24 hours, respectively. The maximum differences decrease considerably with the forecast, especially for the height field. The changes in the height and wind fields for INMI and ENMI, as seen from table 2, show quantitatively the similarity between INMI and

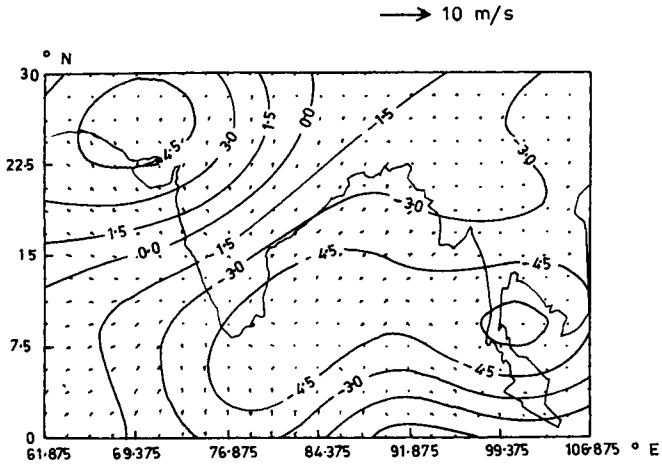

Figure 11. Difference in 24-hour forecast of wind and height fields between ENMI and NOIN starting from the dataset at 500 mb on July 6th 1979 (12 UTC).

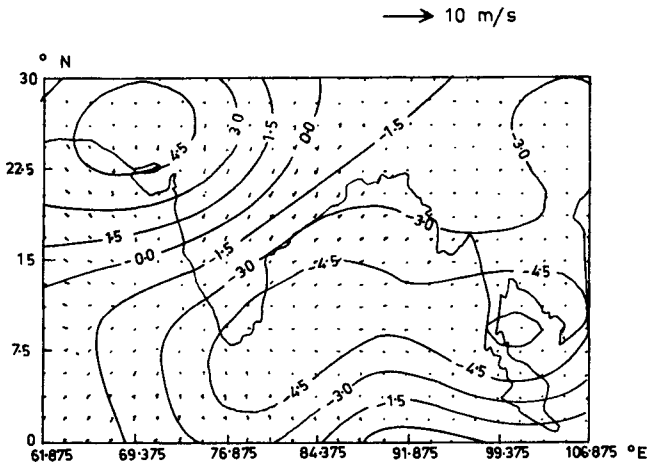

Figure 12. Difference in 24-hour forecast of wind and height fields between INMI and NOIN starting from the dataset at 500 mb on July 6th, 1979 (12 UTC).

ENMI at the initial stage as well as after several hours of forecast.

The 24-hour forecasts of wind and height fields starting from the uninitialized data, ENMI data and INMI data are shown in figures 8, 9 and 10, respectively. Figures 9 and 10 are virtually identical to one another and are also similar to the forecast from the uninitialized data (figure 8). The circulation centre remains unaltered in all the three figures (figures 8, 9 and 10) having the same value of height field (5828 m). The difference in 24-hour forecast of wind and height field between the initialized and uninitialized data is shown in figure 11 (for ENMI) and figure 12 (for INMI). These two difference plots are indistinguishable from each other. Also it is observed that the magnitude of this forecast difference field has decreased markedly compared to the initial difference field (figure 6 and 7).

4.4 *Computational time*

Finally, the computational times of both the schemes are compared. However the computation time depends on the number of iterations required to implement the schemes. As shown in table 1, there is very little change in the rms difference value of wind components and height value with the iteration number. However it was observed that for both the initialization schemes the maximum changes to the initial fields of height and wind component for one and two iterations were not very small. For three iterations, the maximum changes in the height and wind components in the initial fields were negligibly small. This led us to conclude that two iterations are sufficient for the initialization scheme.

The CPU times in seconds for execution (in Cyber 180/840A) of the two schemes are tabulated in table 3. It is found ENMI takes more time than INMI for 2 iterations though the difference decreases with increasing iteration number. This is because ENMI takes more time for computing and storing normal modes, but once it is stored it can be used for further iterations.

5. Conclusions

The results of an experiment with both explicit and implicit nonlinear normal mode initialization for a tropical region have been presented. Both explicit and implicit initialization schemes are capable of eliminating the unwanted gravity wave oscillation and only make small changes to the initial field without affecting the forecast. They are virtually identical in their effect upon the initial field.

However the INMI scheme appears more attractive than the ENMI scheme as it requires less computational time and also does not depend on the geometry of the model. So it may be applicable to most of the limited area models unlike the ENMI scheme.

Table 3. *CPU time for execution of the schemes with different iterations.*

	Schemes	One iteration	Two iterations	Three iterations
CPU (sec)	INMI	10.18	18.91	27.65
	ENMI	22.08	27.57	33.08

Acknowledgements

Authors are indebted to Prof. K L Chopra for his kind encouragement. Many helpful comments of the referees are gratefully acknowledged.

References

Andersen J H 1977 A routine for normal mode initialization with nonlinear correction for a multi-level spectral model with triangular truncation; European Center for Medium Range Weather Forecasts; *Internal Rep. No. 15* 41 pp

Bijlsma S J and Hafkenscheid L M 1986 Initialization of a limited-area model: A comparison between the nonlinear normal mode and bounded derivative methods; *Mon. Weather Rev.* **114** 1445–1455

Bourke W and McGregor J L 1983 A nonlinear vertical mode initialization scheme for a limited-area prediction model; *Mon. Weather Rev.* **111** 2285–2297

Briere S 1982 Nonlinear normal mode initialization of a limited area model; *Mon. Weather Rev.* **110** 1166–1186

Daley R 1979 The application of nonlinear normal mode initialization to an operational forecast model; *Atmos. Ocean* **17** 97–124

Davies H C 1983 Limitations of some common lateral boundary schemes used in regional NWP models; *Mon. Weather Rev.* **111** 1002–1012

Juvanon du Vachat R 1986 A general formulation of the normal modes for limited area models: Application to initialization; *Mon. Weather Rev.* **114** 2478–2487

Juvanon du Vachat R 1988 Non-normal mode initialization: Formulation and application to inclusion of the β terms in the linearization; *Mon. Weather Rev.* **116** 2013–2024

Kasahara A 1982 Nonlinear normal mode initialization and the bounded derivative method; *Rev. Geophys. Space Phys.* **20** 385–397

Krishnamurti T N, Kumar A, Yap K S, Dastoor A P, Davidson N and Sheng J 1990 Performance of a high-resolution mesoscale tropical prediction model; *Advances in Geophysics* Academic Press **32** 133–286

Machenhauer B 1977 On the dynamics of gravity oscillations in a shallow water model, with application to normal mode initialization; *Beitr. Phys. Atmos.* **50** 253–271

Nair D R C, Chakravarty B and Niyogi P 1993a Implicit nonlinear normal mode initialization for a barotropic primitive equation limited area model; *Mausam* **44** 1–8

Nair D R C 1993b Studies on initialization of a tropical semi-lagrangian semi-implicit numerical weather prediction model. PhD thesis, Indian Institute of Technology (Kharagpur, India)

Sadourny R 1975 The dynamics of finite difference models of the shallow water equations; *J. Atmos. Sci.* **32** 680–689

Temperton C and Williamson D L 1981 Normal mode initialization for a multilevel gridpoint model, Part I: Linear aspects; *Mon. Weather Rev.* **109** 729–743

Temperton C 1988 Implicit normal mode initialization; *Mon. Weather Rev.* **116** 1013–1031

Temperton C 1989 Implicit normal mode initialization for spectral models; *Mon. Weather Rev.* **117** 436–451

Temperton C and Roch M 1991 Implicit normal mode initialization for an operational regional model; *Mon. Weather Rev.* **119** 667–677

MS received 2 August 1994; revised 17 October 1996